Deformation of Fields Propagating Through Gas Lenses

By D. MARCUSE

(Manuscript received June 23, 1966)

The concept of a thin lens equivalent to a gas lens is used to calculate distortions of off-axis Gaussian fields in beam waveguides composed of gas lenses. A computational method for the numerical solution of this problem based on the Kirchoff-Huygens diffraction integral is developed. It is shown that off-axis Gaussian fields deform considerably as they travel through a sequence of gas lenses. These deformations are substantial even though the lens distortions may be small. If the light beam deforms it is hard, if not impossible, to steer it back on-axis. This problem can be avoided if some means of beam redirection are used to keep the field on-axis, thus preventing the occurrence of significant beam deformation.

I. INTRODUCTION

Interest in optical communications has stimulated research to find a suitable optical transmission medium. The beam waveguide first suggested by Goubau[1] appears to be an efficient optical waveguide. It is composed of lenses which periodically refocus the light beam, counteracting its tendency to spread apart by diffraction.

Gas lenses have been suggested as focusing elements of beam waveguides.[2,3,4] Of the various types of gas lenses, the tubular gas lens, Fig. 1(a), has been studied in some detail.[3,4] This gas lens can be represented by an equivalent thin lens which is warped to fit the shape of the principal surface of the gas lens and which is given its focal length with the proper dependence on its radius. It was shown in Ref. 5 that ray trajectories through 100 gas lenses coincide closely with ray trajectories through the corresponding equivalent lenses. Replacing the complicated gas lens with the equivalent thin lens simplifies considerably the study of beam waveguides composed of gas lenses.

In this paper, we will make use of the equivalent thin lens concept to investigate the propagation of wave fields through a beam waveguide of

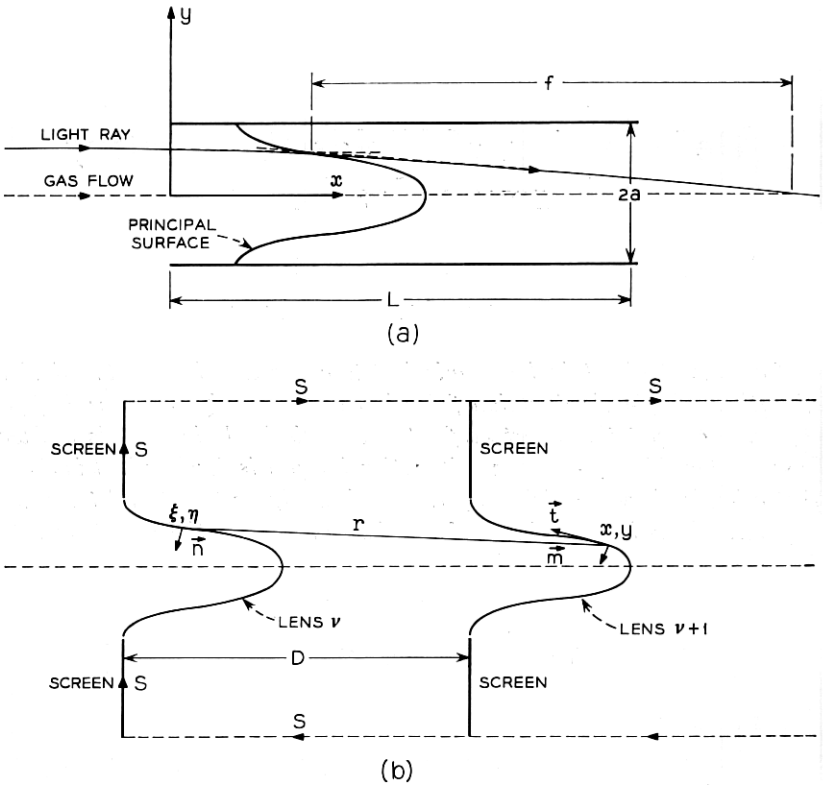

Fig. 1— (a) Schematic of the gas lens indicating the definition of principal surface and focal length. (b) The equivalent warped, thin lenses representing the gas lens beam waveguide.

gas lenses. The justification for replacing the gas lenses with equivalent lenses comes from geometric optics.[5] One might wonder if the argument based on geometric optics can be carried over into wave optics. The geometric optics description neglects diffraction effects. Inasmuch as diffraction effects can be neglected as the field passes through the lens, the geometric optics description should give the correct answer. Based on this line of reasoning, one may expect the equivalent thin lens to be a good approximation, as long as the gas lenses are short compared to their spacing.

The wave optics properties of the beam waveguide composed of gas lenses are obtained using a two-dimensional version of the scalar Kirchoff-Huygens diffraction integral. The problem had to be limited to two

dimensions to make it tractable for computer calculations. This simplification can be visualized as replacing the actual lenses by cylindrical lenses.

We study how off-axis field distributions with a Gaussian intensity profile propagate through the beam waveguide. Unfortunately there are further limitations on the physical problem we can compute, imposed by the limited size of the available computer memory. The calculations are accelerated if as much of the integral kernel as possible can be stored in the machine without having to recalculate it each time it is needed. The IBM 7094 used for these calculations has 24,000 storage locations available in its memory. Since we are dealing with a complex kernel, 100 integration points across the (linear) lens require 20,000 storage locations. This means that we can use no more than 100 integration points to compute our problem. This limits the ratio of lens aperture to field extension across the lens which we can use. Either we use the full lens aperture and launch a field which fills an appreciable part of it or we use a very narrow field distribution and limit the aperture to a size which allows us to approximate the narrow field reasonably well with the 100 integration points at our disposal. This limitation forced me to calculate the field distribution in the gas lens either at a much lower frequency than that of the visible 6328Å line of a He-Ne laser or to take the actual laser frequency but use only a small fraction of the actual lens aperture.

In spite of all these limitations imposed by computer economics, some interesting results can still be obtained.

In a beam waveguide composed of ideal lenses no field distortion results as an off-axis Gaussian beam travels through the waveguide. In a beam waveguide composed of gas lenses, off-axis Gaussian beams break up into double humped shapes and deform so much that it is hard to locate the initially well defined field distribution. This result is important for beam waveguides using electronic control mechanisms to reposition a beam when it has wandered away from the waveguide axis.[6] If the beam breaks up into several beams, repositioning becomes impossible. This problem can be minimized by using two gas lenses back-to-back close together. The resulting combined lens has far less principal plane distortion as the individual lenses and leads to far less field distortion.

The field distortion observed in these simulated gas lenses can be attributed in part to the distortion of the principal plane. A fictitious lens with the same focal length aberration as the gas lens but an undistorted principal plane shows less field distortion. However, the focal length aberration also contributes its share of field distortions.

A large part of this paper is taken up with the description of the calculation procedure. This is justified since the development of a workable and logical procedure is perhaps the main contribution of this work. The reader who is interested only in the numerical results may skip over the following two sections to the section entitled "Discussion of Numerical Results."

II. THE TWO-DIMENSIONAL DIFFRACTION INTEGRAL

The Kirchoff-Huygens diffraction integral is a solution of the scalar wave equation.

$$\Delta\Psi + \beta^2\Psi = 0. \tag{1}$$

As explained in the introduction, we are not interested here in the three-dimensional case usually treated but in its two-dimensional counterpart. The two-dimensional Kirchoff-Huygens integral is

$$\Psi(x,y) = \frac{i}{4}\int_s \left\{\frac{\partial\Psi}{\partial n} H_o^{(1)}(\beta r) - \Psi \frac{\partial}{\partial n} H_o^{(1)}(\beta r)\right\} dS. \tag{2}$$

The integral is to be extended over a closed curve S, n indicates the direction of the normal to the curve S which counts positive if it points outward of the area enclosed by S. $H_o^{(1)}$ is the Hankel function of zero order and first kind. The variable r is the distance between the observation point x,y inside of S and the integration point ξ, η on S,

$$r = \sqrt{(x-\xi)^2 + (y-\eta)^2}. \tag{3}$$

dS is the line element along the curve S. The constant β is related to the wavelength λ of the radiation field by

$$\beta = \frac{2\pi}{\lambda}. \tag{4}$$

We are dealing with an optical radiation field. The observation point x,y will always be far enough from the line S so that

$$\beta r \gg 1.$$

It is, therefore, possible to replace the Hankel function by its approximation for large argument and write (2)

$$\Psi(x,y) = \frac{\exp\left(i\frac{\pi}{4}\right)}{\sqrt{8\pi\beta}} \int_s \left\{\frac{\partial\Psi}{\partial n}\frac{\exp(i\beta r)}{\sqrt{r}} - \Psi\frac{\partial}{\partial n}\left(\frac{\exp(i\beta r)}{\sqrt{r}}\right)\right\} dS. \tag{5}$$

Equation (5) relates the values of the field $\Psi(\xi,\eta)$ on S to its values inside S. We want to use this expression to calculate the field at lens $n+1$ if the field at lens n is known. Our lenses are the equivalent thin lenses of Fig. 1 (b) which represent the gas lens of Fig. 1 (a). The fields have to be known over the surface of the lens which is not plane. We assume that the lens is apertured by an opaque screen and follow the usual practice of setting

$$\Psi(\xi,\eta) = 0 \quad \text{and} \quad \frac{\partial \Psi}{\partial n} = 0 \tag{6}$$

on the screen. We use as the curve S the line formed by the lens surface. the opaque screen which extends from $-\infty < \eta < \infty$, and close it by a suitable curve at infinity. The following lens of the beam waveguide lies thus inside S, Fig. 1 (b).

The Kirchoff-Huygens integral presents a problem. It requires us to know not only Ψ on S but also $\partial\Psi/\partial n$. It is not sufficient, therefore, to simply evaluate the integral (5) but also the integral which follows from it by differentiation with respect to the normal $\mathbf{m}$ to the surface of the next lens in the beam waveguide.

A substantial simplification results if instead of Ψ we use a function Φ defined by the equation

$$\Psi = \Phi e^{i\beta x}. \tag{7}$$

This transformation serves the following purpose. The field propagating in the beam waveguide can be expected to have phase fronts which are not too different from that of plane waves. Since we collect the field over the curved surface of the lenses we have a substantial phase variation simply because the curved surface crosses many phase fronts of the almost plane wave. The transformation (7) displays explicitly the plane wave part of the phase variation. The remaining phase variation left in Φ is much less rapid and therefore much easier to calculate. Substituting (7) into (5) leads to an equation for Φ. We also replace the phase constant β by

$$\beta = 2\pi N \frac{D}{a^2} \tag{8}$$

with

$$N = \frac{a^2}{D\lambda}. \tag{9}$$

N is the Fresnel number which is often used to characterize optical

resonators and beam waveguides. D is the distance between lenses and "a" the half-width of their apertures.

Replacing Ψ by Φ introduces the term $\exp[i\beta(r + \xi - x)]$ under the integral sign. We make use of the fact that $x - \xi$ is almost as large as r and write approximately

$$r + \xi - x = \frac{1}{2}\frac{(y-\eta)^2}{x-\xi}\left\{1 - \frac{1}{4}\left(\frac{y-\eta}{x-\xi}\right)^2\right\}. \tag{10}$$

Using (7), (8), and (10) we can rewrite (5)

$$\begin{aligned}\Phi_{\nu+1}(y) = \frac{\sqrt{ND}}{2a}\exp\left(-i\frac{\pi}{4}\right)\int_{-a}^{a}\left\{\left(\frac{\partial r}{\partial n} - \frac{\partial \xi}{\partial n}\right)\Phi_\nu(\eta)\right.\\ \left. + \varphi_\nu(\eta)\right\}\frac{\sqrt{1+\left(\frac{d\xi}{d\eta}\right)^2}}{\sqrt{r}}\\ \cdot\exp\left[i\pi N\frac{D}{a^2}\frac{(y-\eta)^2}{x-\xi}\left\{1 - \frac{1}{4}\left(\frac{y-\eta}{x-\xi}\right)^2\right\}\right]d\eta.\end{aligned} \tag{11}$$

The line element dS was expressed by

$$dS = \sqrt{1+\left(\frac{d\xi}{d\eta}\right)^2}\,d\eta \tag{12}$$

where $\eta = \eta(\xi)$ or $\xi = \xi(\eta)$ is the function describing the curved lens. The function $\varphi_\nu(\eta)$ is defined by

$$\varphi_\nu(\eta) = \frac{i}{\beta}\frac{\partial \Phi_\nu(\eta)}{\partial n}. \tag{13}$$

The subscripts ν and $\nu + 1$ have been added to underscore the iterative nature of the process.

The iterative equation for the calculation of $\varphi_{\nu+1}$ follows from $\Phi_{\nu+1}$ by differentiation. Neglecting certain small terms under the integration sign results in

$$\begin{aligned}\varphi_{\nu+1}(y) = \frac{\sqrt{ND}}{2a}\exp\left(-i\frac{\pi}{4}\right)\int_{-a}^{a}\left\{\frac{1}{2}\left(\frac{y-\eta}{x-\xi}\right)^2\frac{\partial x}{\partial m} - \frac{y-\eta}{x-\xi}\frac{\partial y}{\partial m}\right\}\\ \cdot\left\{\left(\frac{\partial r}{\partial n} - \frac{\partial \xi}{\partial n}\right)\Phi_\nu(\eta) + \varphi_\nu(\eta)\right\}\frac{\sqrt{1+\left(\frac{d\xi}{d\eta}\right)^2}}{\sqrt{r}}\\ \cdot\exp\left[i\pi N\frac{D}{a^2}\frac{(y-\eta)^2}{x-\xi}\left\{1 - \frac{1}{4}\left(\frac{y-\eta}{x-\xi}\right)^2\right\}\right]d\eta.\end{aligned} \tag{14}$$

The symbol m was used to designate the normal of the $(\nu + 1)$th surface $y = y(x)$.

For reasons explained later, we also need the derivation of Φ in tangential direction t. Defining

$$\chi = \frac{i}{\beta} \frac{\partial \Phi}{\partial t} \tag{15}$$

we get the integral expression for $\chi_{\nu+1}$ by replacing $\partial/\partial m$ by $\partial/\partial t$ in (14), it is unnecessary to write this expression down since it is exactly the same as that for $\varphi_{\nu+1}$ except for the change just mentioned.

The three integrals for Φ, φ, and χ have a substantial part of their integrands in common. This similarity facilitates the machine calculations of these integrals greatly.

The power flow through the lenses can be computed from the expression[7]

$$P_\nu = \frac{\omega}{2} \int_{S_\nu} Im(\Psi \nabla \Psi^*) dS \tag{16}$$

with ω being the angular frequency of the radiation field and Im denoting the imaginary part of the expression in parenthesis. Or replacing Ψ by Φ and the line element by (12) we get with the help of (13)

$$P_\nu = \frac{\omega\beta}{2} \int_a^a \left\{ \mathrm{Re}\,(\Phi_\nu \varphi_\nu^*) - \frac{\partial \xi}{\partial n} |\, \Phi_\nu \,|^2 \right\} \sqrt{1 + \left(\frac{d\xi}{d\eta}\right)^2}\, d\eta. \tag{17}$$

Equation (17) can be used to compute the power flow through the lenses and observe power loss due to diffraction caused by the finite lens apertures.

The reader who is familiar with the work of Fox and Li[8] might wonder why the present case is so much harder to compute than the resonators studied by these authors. Fox and Li used only one integral to describe the field distribution over one mirror in terms of the field distribution over the other, they did not calculate the integral for $\partial\Psi/\partial n$ simultaneously with that for Ψ. The reason for the success of the much simpler theory in their case was the fact that the surfaces over which they had to integrate were either perfectly flat or very nearly plane. The normal derivatives occurring in (2) involve the cosines of angles ε between the normal to the surface of integration and the normal to the phase fronts of the wave. As long as this angle is small

$$\cos \varepsilon \approx 1$$

and the angle can be ignored. For the purpose of the normal derivative

the wave can be treated as perfectly plane and the derivative can be written as

$$\frac{\partial \Psi}{\partial n} = i\beta\Psi. \tag{18}$$

However, the angle α between the direction normal to the surface of our lenses and the optical axis is not small. If ε is again the angle between the normal to the phase front of the wave and the optical axis then $\alpha + \varepsilon$ is the angle entering the cosine. But even if ε is small

$$\cos(\alpha + \varepsilon) \approx \cos\alpha - \varepsilon \sin\alpha.$$

The departure of the phase front from a plane wave can no longer be neglected but enters in first order. The expression (18) is no longer a valid approximation and the whole calculation becomes much more difficult.

III. FIELD TRANSMISSION THROUGH THE LENSES

So far we have considered the transmission of the field from the surface of one lens to that of the next. However, the lenses have so far not even entered the picture other than to force us to calculate the field over the surface of the lens. The process of calculating the effect of the lens on the field is also rather complicated. In the case of plane, thin lenses it is sufficient to regard the lens simply as a phase transformer which retards the phase of the field differently in different parts of the lens. This simple picture is inapplicable in our case of curved lenses.

Liouville's theorem of statistical mechanics is the guide to the proper description of a thin lens. I have shown in two earlier papers[5,9] how rays pass through thin lenses. The ray gets broken by the lens by an angle which depends not only on the part of the lens which the ray intersects, but also by the angle between the ray and the normal to the lens surface. If γ_1 is this angle for the entering ray and γ_2 that for the ray leaving the lens the dependence between these two angles is given by[9]

$$\sin\gamma_2 = \sin\gamma_1 + F(y). \tag{19}$$

The function $F(y)$ is determined by the lens. The focusing property of the lens determines the angle γ_2' if γ_1' corresponds to a ray incident parallel to the optical axis. γ_1' and γ_2' are known from the desired focal length of the lens and its shape. $F(y)$ is determined by substituting $\gamma_2 = \gamma_2'$ and $\gamma_1 = \gamma_1'$ into (19).

These ray optics properties of the lens have to be used to determine its influence on the field. The normal directions to the phase fronts coin-

cide with the rays associated with the field, they have to be determined from the derivatives of the field function. Let us assume that we split the field function Ψ into its magnitude G and phase angle $\beta\vartheta$

$$\Psi = G \exp (i\beta\vartheta)$$

or using Φ rather than Ψ

$$\Phi = G \exp [i\beta(\vartheta - x)]. \tag{20}$$

The function $\vartheta(x,y)$ is the eikonal of geometric optics and satisfies the eikonal equation of free space[10]

$$| \nabla\vartheta | = 1. \tag{21}$$

We take the tangential derivative of Φ

$$\frac{\partial\Phi}{\partial t} = \left[i\beta \left(\frac{\partial\vartheta}{\partial t} - \frac{\partial x}{\partial t} \right) + \frac{\partial G}{\partial t} \frac{1}{G} \right] \Phi. \tag{22}$$

The term $\partial\vartheta/\partial t$ can be expressed in the following way

$$\frac{\partial\vartheta}{\partial t} = \nabla\vartheta \cdot \frac{\partial \mathbf{s}}{\partial t} = | \nabla\vartheta | \left| \frac{\partial \mathbf{s}}{\partial t} \right| \cos (kt);$$

$\partial\mathbf{s}/\partial t$ is a unit vector in the tangential direction t, (kt) is the angle between the direction normal to the phase front of the wave and the tangential direction. Using (21) and the property of the unit vector we obtain

$$\frac{\partial\vartheta}{\partial t} = \cos (kt). \tag{23}$$

With the help of (15) and (23) we get from (22)

$$\cos (kt) = \frac{\partial x}{\partial t} - \frac{\chi}{\Phi} + \frac{i}{\beta} \frac{1}{G} \frac{\partial G}{\partial t}.$$

The left-hand side of this equation is real by definition and so is G and its derivatives. This means that the imaginary parts of the right-hand side have to cancel each other and we obtain

$$\cos (kt) = \frac{\partial x}{\partial t} - \mathrm{Re} \left(\frac{\chi}{\Phi} \right). \tag{24}$$

Re designates the real part of the expression in parentheses. The derivative $\partial x/\partial t$ is known from the geometry of the lens, and χ as well as Φ have been computed from their integral expressions. The angle between the rays associated with the field and the tangential direction t of the

curve describing the lens shape is thus determined. The angle (kt) is related to γ_1, the angle between the ray and the normal to the lens surface, by

$$\gamma_1 = \frac{\pi}{2} - (kt) \tag{25}$$

so that

$$\cos (kt) = \sin \gamma_1 .$$

The angle γ_2 between output ray and lens normal is obtained from (19). Indicating by a prime the angles and field quantities of the field after leaving the lens we have

$$\cos (kt)' = \sin \gamma_2$$

and from (23)

$$\vartheta' = \int_{t_1}^{t} \cos (kt)' \, dt \tag{26}$$

or

$$\Delta\vartheta = \vartheta' - \vartheta = \int_a^y [\cos (k't) - \cos (kt)] \sqrt{1 + \left(\frac{dx}{dy}\right)^2} \, dy. \tag{27}$$

The transformed field after it has passed the lens can now be calculated

$$\Phi_{\nu+1}' = \Phi_{\nu+1} \exp (i\beta\Delta\vartheta). \tag{28}$$

Finally, we need to know the normal derivative $\varphi_{\nu+1}'$ of $\Phi_{\nu+1}'$ before we are ready for the next iteration step. Replacing derivatives with respect to t by the normal derivatives with respect to m in (22) and multiplying by i/β we obtain

$$\varphi_{\nu+1} = \left[\frac{\partial x}{\partial m} - \frac{\partial \vartheta}{\partial m} + \frac{i}{\beta}\frac{1}{G}\frac{\partial G}{\partial m}\right]\Phi_{\nu+1} . \tag{29}$$

The derivative $\partial\vartheta/\partial t$ was equal to $\cos (kt)$, similarly we can write

$$\frac{\partial \vartheta}{\partial m} = \cos (km). \tag{30}$$

The angle (km) is related to γ_1 by

$$(km) = \pi - \gamma_1 .$$

The reader might wonder why I bothered introducing the angle (kt) and the derivative χ since $\partial\vartheta/\partial m$ which is determined by φ gives the

angle γ_1 directly. However, $\partial\vartheta/\partial m$ only determines $\cos\gamma_1$. The conversion of $\cos\gamma_1$ to $\sin\gamma_1$ leaves the sign of γ_1 ambiguous. No such ambiguity arises if (kt) is computed.

The angle $(km)'$ belonging to the output field can now easily be obtained with the help of (19) and (24)

$$\frac{\partial\vartheta'}{\partial m} = \cos(km)' = -\sqrt{1-\sin^2\gamma_2}\,. \tag{31}$$

Substituting (31) into (29) written for the primed quantities we get

$$\varphi_{\nu+1}' = \left[\frac{\partial x}{\partial m} - \cos(km)' + \frac{i}{\beta}\frac{1}{G}\frac{\partial G}{\partial m}\right]\Phi_{\nu+1}'$$

or using (29) once more and keeping in mind (28)

$$\varphi_{\nu+1}' = \varphi_{\nu+1}\exp(i\beta\Delta\vartheta) + [\cos(km) - \cos(km)']\varphi_{\nu+1}'. \tag{32}$$

The transformed field quantities of (28) and (32) are certain to conform with the requirements of ray optics. However, this is not quite sufficient to satisfy all the wave optics requirements. Numerical results have shown that the fields Φ' and φ' substituted into the power formula (17) yield a different number for the power flow than the one obtained from using (17) with Φ and φ. The fields Φ' and φ' after having passed the lens should carry the same amount of power as the input fields. The transformation procedure, outlined so far, takes into account the phase of the field and the change in slope of the phase fronts in accordance with physical principles but it does not account for any change in field amplitude which the physics of the (lossless) lens might also require. In fact, the failure of this transformation to obey conservation of energy points to a need to readjust the field amplitudes. To correct the amplitudes of the field quantities Φ' and φ' locally, I computed the ratio of the integrals of (17) taken with the two fields. Letting I be the integrand of (17) calculated with the use of Φ and φ, and I' the corresponding value obtained using Φ' and φ', I calculated

$$R = \sqrt{\frac{I}{I'}} \tag{33}$$

and introduced

$$\Phi'' = R\Phi'$$

and (34)

$$\varphi'' = R\varphi'.$$

This last transformation does not affect the phase of the field or its slope but adjusts the field amplitude so that using Φ'' and φ'' the power is conserved in the process of transmitting the field through the infinitely thin and lossless lens. This last transformation does not transform away diffraction losses, however, since those occur in passing the field from one lens to the next.

This completes the description of the iteration procedure. It is surprising how much the calculation is complicated by the simple fact that the lenses are not plane but curved. One might regard the simplicity of the plane lenses as a lucky break. The present procedure naturally is more time consuming. To pass the field through 100 lenses of the lens waveguide with plane lenses using the simple procedure of Fox and Li takes 0.023 hours of 7094 computer time. The procedure described above takes 0.13 hours for the same number of lenses or 5.65 times as long. The present procedure is that much more involved.

IV. DISCUSSION OF NUMERICAL RESULTS

The calculation procedure described on the previous pages was used to study the fate of an off-axis field distribution as it propagates through the beam waveguide. In a beam waveguide composed of ideal, thin lenses the field would suffer no distortions as it travels through the lenses provided that its shape corresponds to a mode of this structure. A mode, even if displaced from the axis, keeps its shape in a perfect beam waveguide. The center of gravity of such an off-axis mode follows the ray trajectory of geometric optics. The field may look somewhat different as it passes different lenses. But whenever its path brings it back to its original position on the lens it assumes the original shape.

This property of ideal lens guides is no longer true for beam waveguides composed of distorting lenses. Now the original field distribution is changed even if the field returns to its original position. These field distortions are best displayed in a motion picture. However, in a paper one has to limit oneself to the display of a few representative frames of such a motion picture.

To launch the field into the waveguide I started with an ideal lens whose focal length corresponded to twice the on-axis focal length of the simulated gas lenses. This procedure was chosen since the modes of the ideal beam waveguide have plane phase fronts right on the lens or in other words after the field has traversed one-half of the lens. A plane phase front and the flat starting lens allow us to take

$$\varphi_o = \frac{i}{\beta}\frac{\partial \Phi_0}{\partial n} = 0$$

so that φ_ν is known initially and the field can get started. On all the following lenses Φ_ν as well as its derivations are calculated.

Figs. 2(a) and 2(b) show the shape of the principal surface p and the focal length f of the lens as functions of position y/a. The function p as well as the focal length f are displayed normalized with respect to the length L of the gas tube. The coordinate y is plotted normalized with respect to the radius a of the tube. These curves correspond to a gas lens operated with a gas velocity which minimizes the focal length at an input gas temperature $T_o = 300°K$, wall temperature of gas tube 355°K, an index of refraction of $n = 1 + 4.210^{-4}$ and a ratio* of $L/a = 50$.

We consider a beam waveguide composed of gas lenses of this type spaced so that $D/f_o = 2$, where D is the distance between adjacent lenses and f_o is the value of the focal length at $y = 0$. Into this beam waveguide we launch a field with a Gaussian intensity profile whose center of gravity is shifted off the optical axis as shown in Fig. 3(a). This field distribution corresponds to a mode of the ideal confocal beam waveguide which is shifted off-axis. The position and shape of this field on the next two lenses is given in Figs. 3(b) and 3(c). Since the beam waveguide is nearly confocal, the center of gravity of the field moves like a ray in a confocal waveguide. No field distortion is yet discernible. Jumping 100 lenses ahead in the beam waveguide we see in Figs. 4(a), 4(b), and 4(c) that the field begins to distort from its original shape. After having traversed 150 lenses the field shows a distinct break-up into two peaks, Fig. 5(a). The appearance of the field on two adjacent lenses can be quite different, Fig. 5(b). Finally, we see the wave field on the lenses 209 and 210 in Figs. 6(a) and 6(b). The distortion has changed somewhat but is not basically different.

The field of Fig. 3(a) fills one-third of the gas lens between the points where it carries more than exp (−2) of its peak power. If we assume a tube with $a = 0.317$ cm (0.125 inch) a waveguide mode of that width corresponds to a light wavelength of $\lambda = 4.60 \times 10^{-4}$ cm which is 7.26 times as long as the wavelength of the 6328Å line of the HeNe laser.

I mentioned in the introduction that the width of the field distribution with respect to the tube radius cannot be made arbitrarily narrow. To consider fields which are similar to modes of the beam waveguide at $\lambda = 6.328 \times 10^{-5}$ cm forces us to reduce the lens aperture. The ratio of field extension and waveguide aperture is maintained if we reduce the wavelength from $\lambda = 4.60 \times 10^{-4}$ cm to $\lambda = 6.328 \times 10^{-5}$ cm and aperture the lens at a value of $y/a = 0.371$ of Figs. 3 through 6. Using only that part of the waveguide between $-0.371 \leqq y/a \leqq 0.371$ and

* These values correspond to $v_0/V = 6.45$ and $C(L/a) = 0.192$ with v_0/V and $C(L/a)$ defined in Ref. 4.

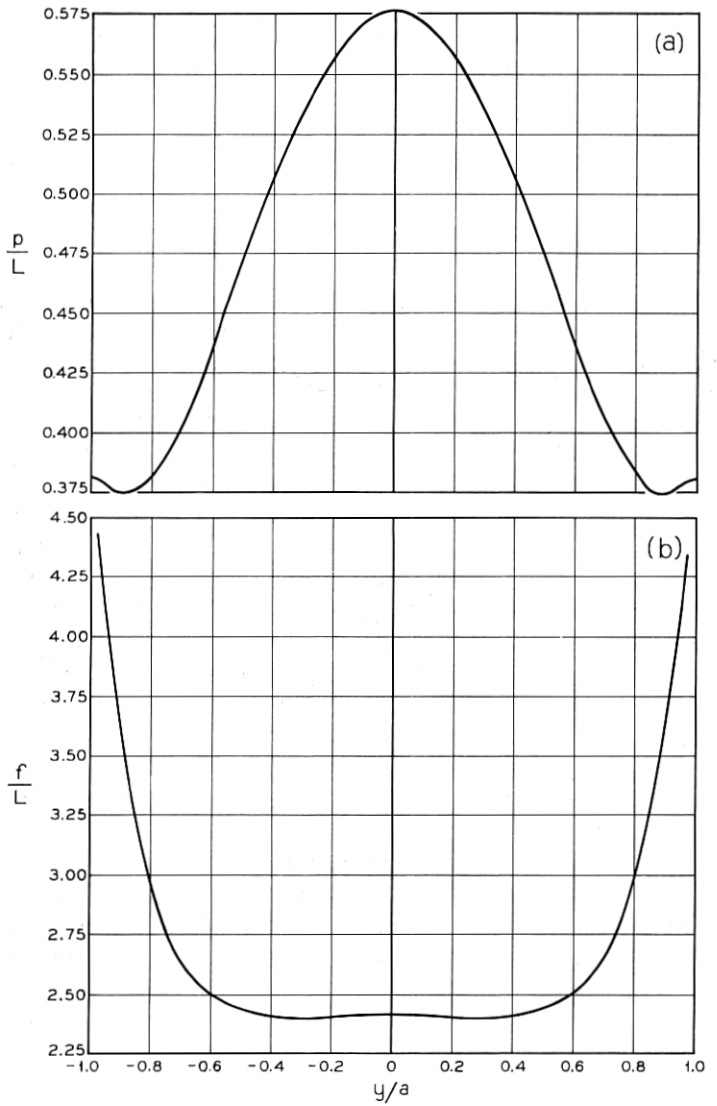

Fig. 2—(a) The principal surface p of the gas lens normalized with respect to the tube length L as a function of y/a. (b) The focal length f of the gas lens normalized with respect to the tube length L as a function of y/a.

renormalizing the y-coordinate so that these boundaries again correspond to $-1 \leqq y/a \leqq 1$ leads to the shape of principal surface and focal length as shown in Figs. 7(a) and 7(b). This is still the same lens, with the only difference that we expanded its center portion. The center portion of the lens has far less distortion as the whole lens of Fig. 2. Figs. 3(a),

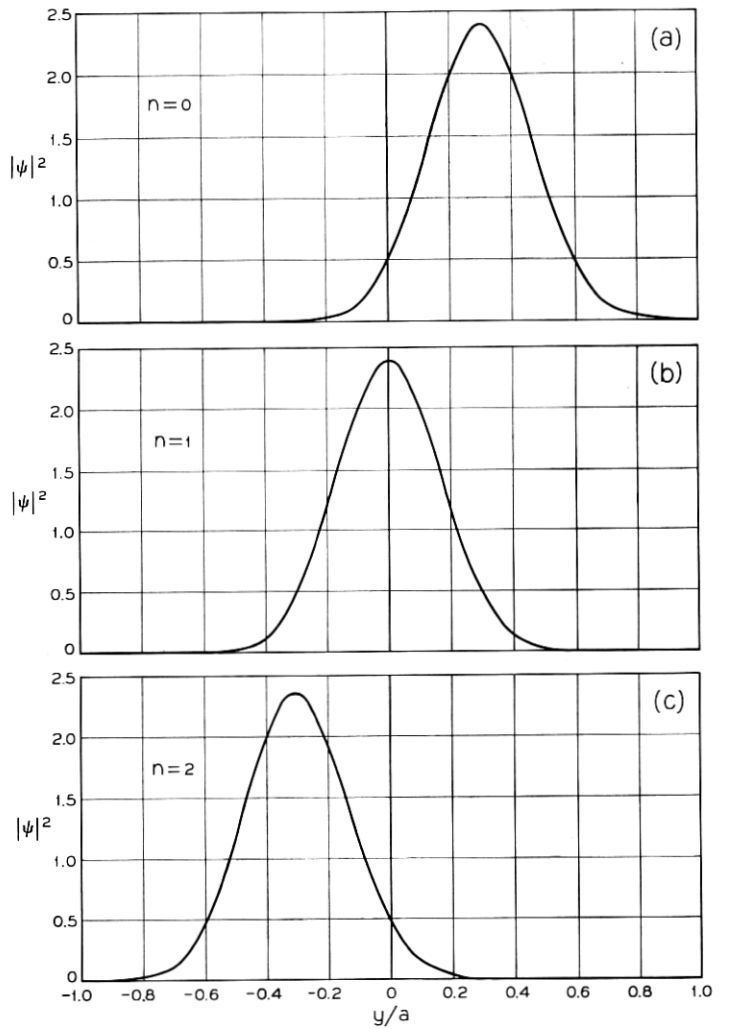

Fig. 3 — The Gaussian field distribution on the first three lenses represented by Fig. 2. The power P carried by the field is $P = 1$.

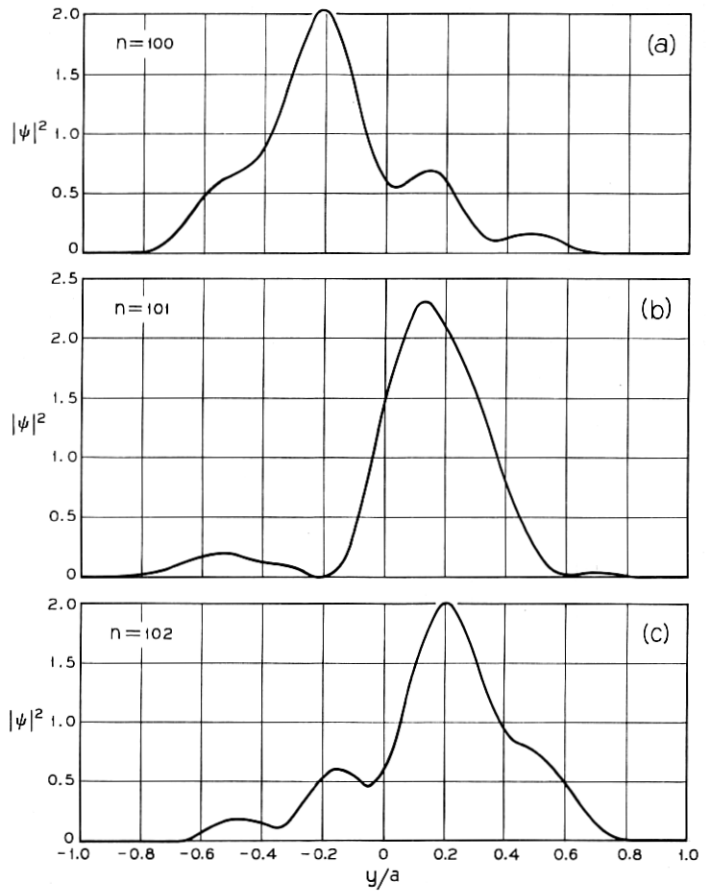

Fig. 4 — The distorted field after passing through 100 lenses $P = 0.969$.

3(b), and 3(c) show again the field distribution on the first three lenses at the wavelength of $\lambda = 6.328 \times 10^{-5}$ cm and the apertured lens. After traversing 120 lenses this field suffered noticeable distortions shown in Figs. 8(a) and 8(b), even though it "sees" now only the center portion of the lens where the focal length depends only very little on y and where the principal surface is much closer to a plane. The dotted curves also shown in these and all remaining figures of field configurations were obtained by maintaining the focal length of the equivalent gas lens, but using a lens with a perfectly flat principal plane. The comparison between the solid and dotted curve shows that the field distortion

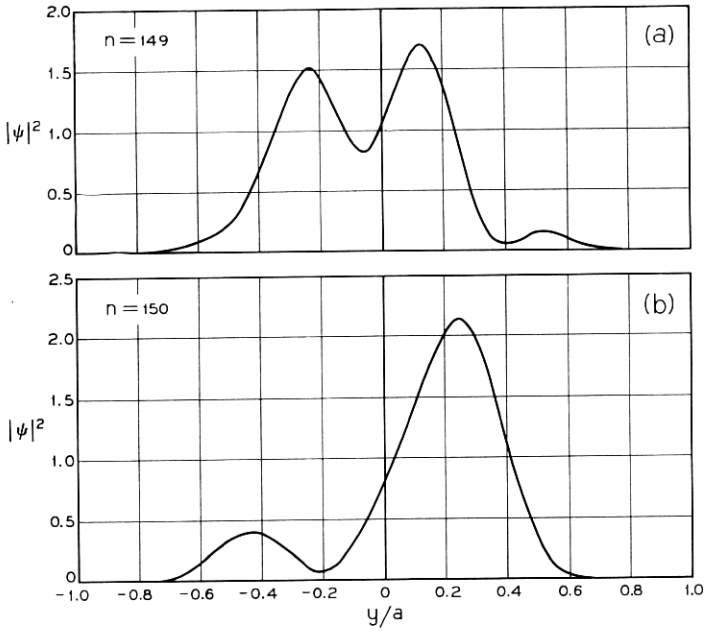

Fig. — 5 Field distortion after 150 lenses. $P = 0.956$.

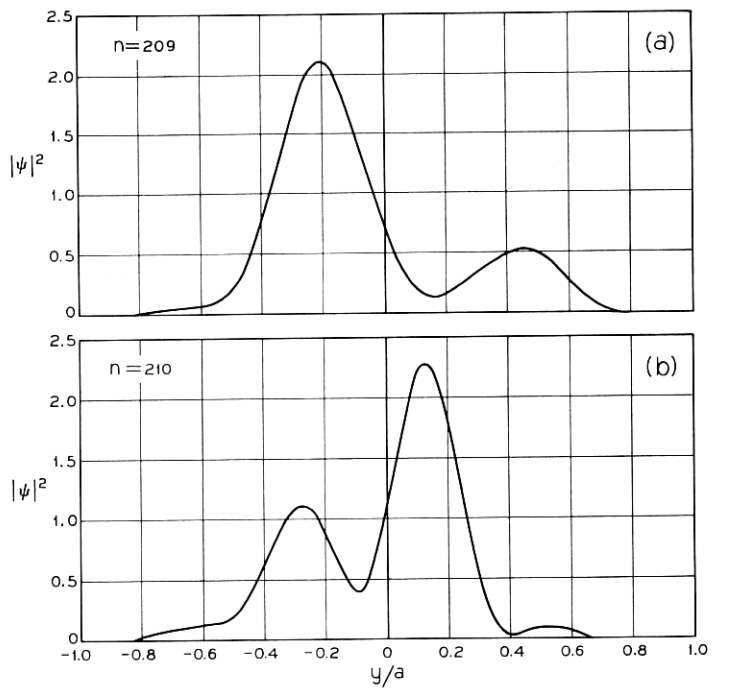

Fig. 6 — Field distortion after 210 lenses. $P = 0.941$.

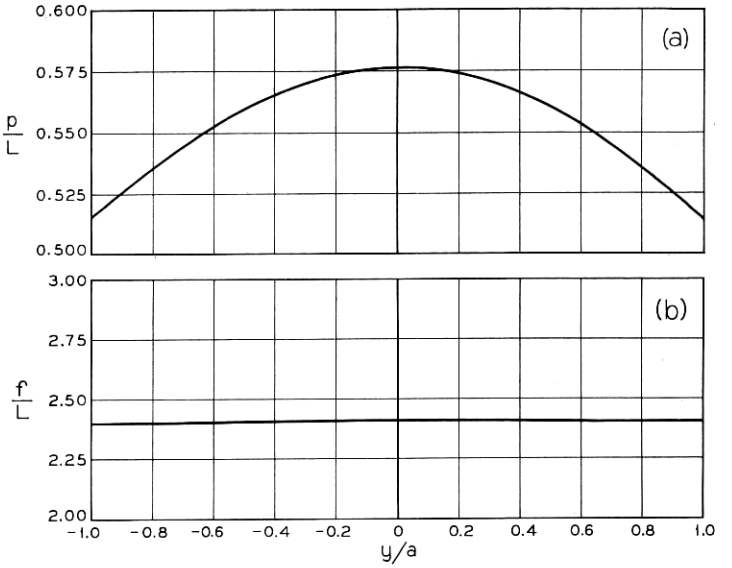

Fig. 7 — (a) Principal surface of the apertured lens. (b) Focal length of the apertured lens.

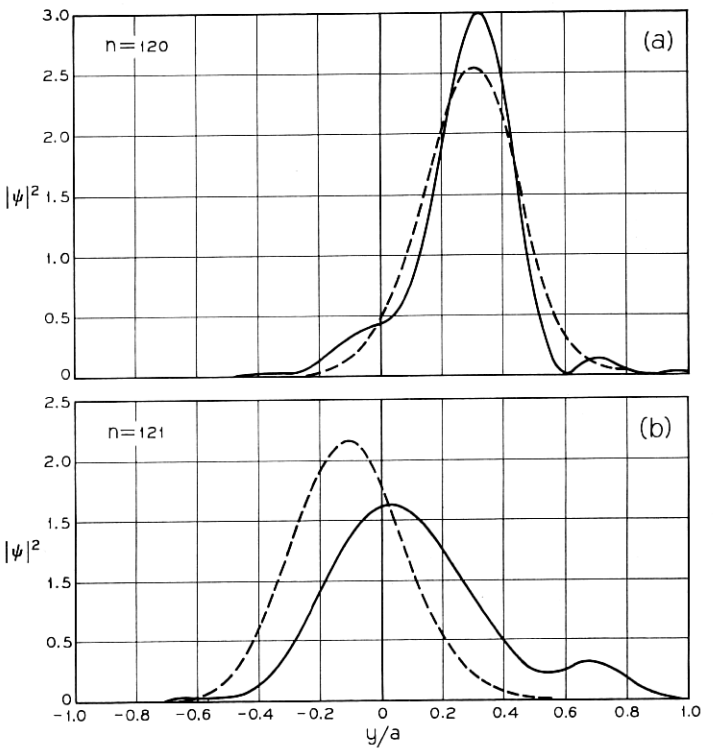

Fig. 8 — Field distortion of the field in the apertured lens after traversing 120 lenses. Solid curves represent the warped thin lens, $P = 0.976$. Dotted curves represent a fictitious plane lens with the same focal length aberration, $P = 1.000$.

can be attributed mainly to the distorted principal plane of this gas lens. The change in width of the field distribution on adjacent lenses as seen in Figs. 8(a) and 8(b) is caused by the departure of the beam waveguide from exact confocality. Figs. 9 and 10 show how bad the field distortions get after 250 and about 400 lenses. Most surprising is the fact that the field distortions of Figs. 8 through 10 are only slightly less severe than those of Figs. 4 through 6, in spite of the substantial improvement of lens aberrations.

To study this point further I constructed a gas lens with even less principal plane distortion by using two gas lenses back-to-back as shown in Fig. 11. The center portion of the principal surface and focal length curve is shown in Figs. 12(a) and 12(b). The expansion and renormalization of these curves is the same as that of Figs. 7(a) and 7(b). The principal surface of this lens, Fig. 11, approximates a plane even better than Fig. 7(a) however, there is more focal length distortion apparent in Fig. 12(b) than in Fig. 7(b). This lens distorts substantially less than

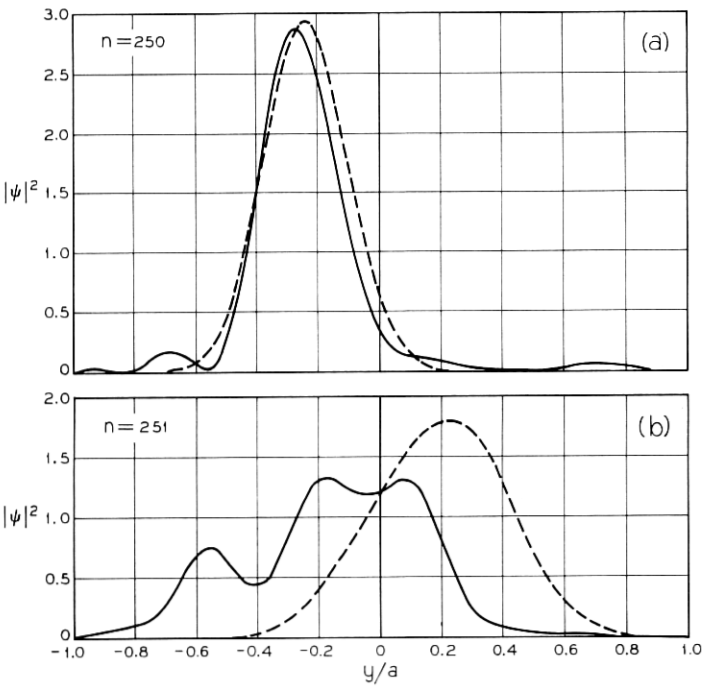

Fig. 9 — Field distortion of the field in the apertured lens after traversing 250 lenses. Solid curve, $P = 0.929$. Dotted curve, $P = 1.000$.

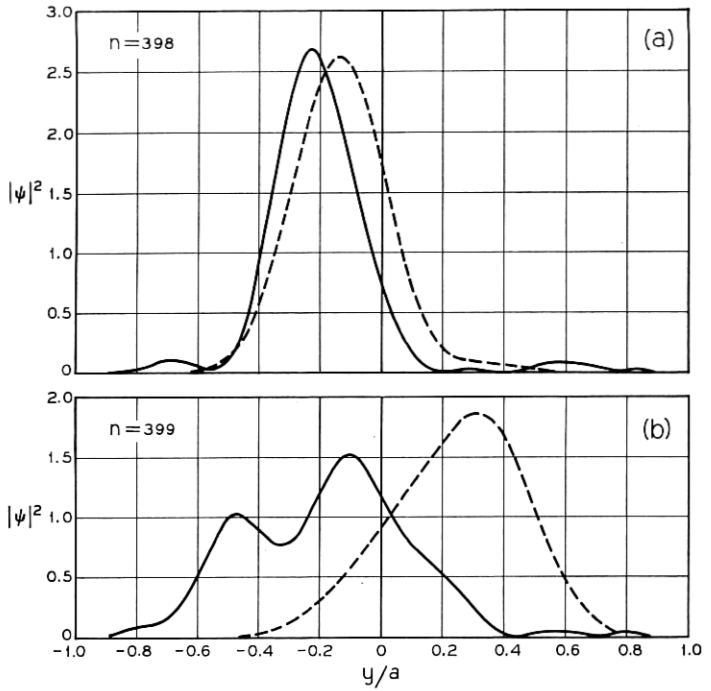

Fig. 10 — Field distortion after 400 lenses. Solid curve, $P = 0.894$. Dotted curve, $P = 1.000$.

the simple lens of Fig. 1, as a comparison of Figs. 8 through 10 with Figs. 13 through 15 indicates. However, even a lens with the characteristics of those shown in Figs. 12(a) and 12(b) causes the field to break up into the double-humped shape of Fig. 16 after traversing 295 lenses.

It is interesting to note the difference between the solid curve and the

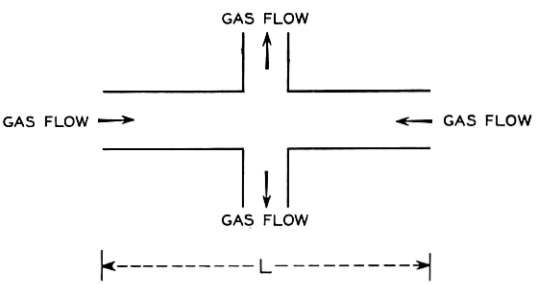

Fig. 11 — Two gas lenses operated back-to-back minimize principal plane distortion.

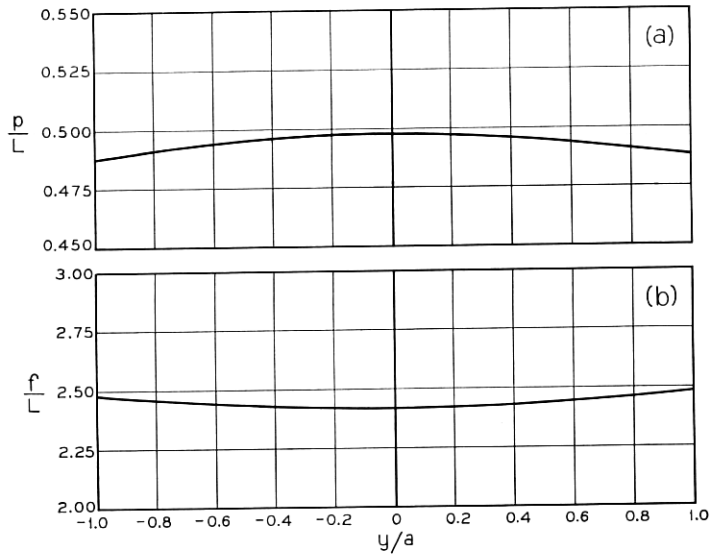

Fig. 12 — (a) Principal surface of gas lens of Fig. 11. (b) Focal length of gas lens of Fig. 11.

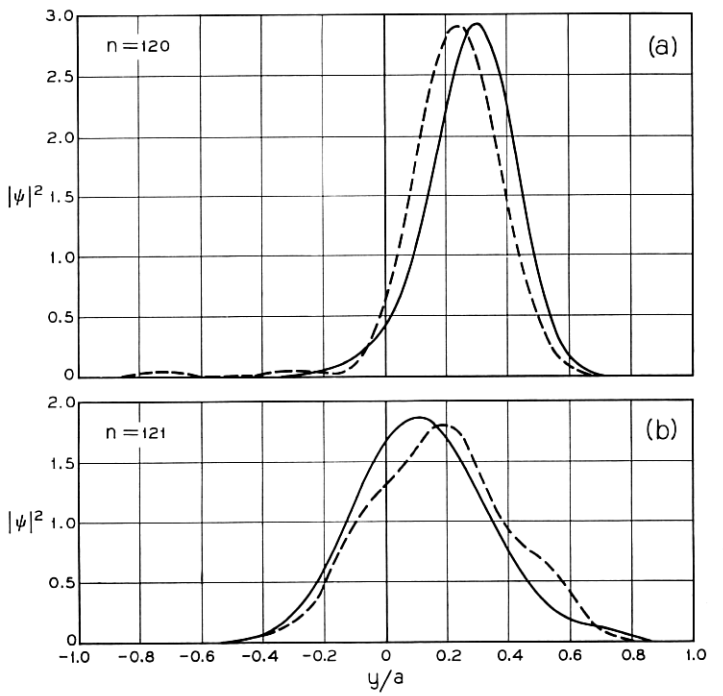

Fig. 13 — Field distortion after 120 lenses. Solid curve represents the lens of Fig. 11, $P = 0.9996$. Dotted curve represents a fictitious plane lens with focal length of Fig. 12(b), $P = 1.0000$.

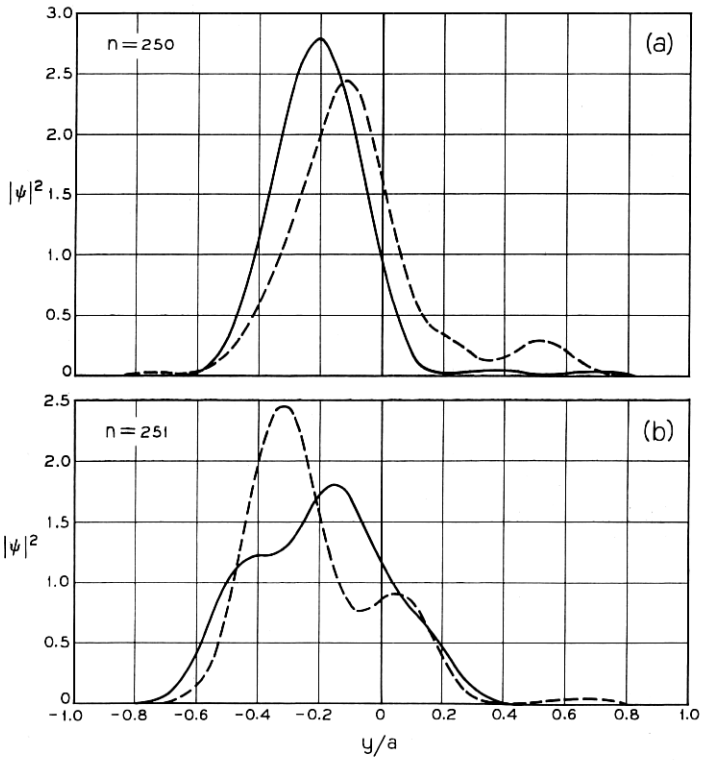

Fig. 14 — Field distortion after 250 lenses. Solid curve, $P = 0.9992$. Dotted curve, $P = 1.0000$.

dotted curve of Figs. 13 through 15. Both curves show field distortions. Those of the solid curves are caused by the combined action of principal plane and focal length distortions, while those of the dotted curves are due to focal length aberration only. It appears that the two distorting influences cancel out to some extent since the solid curves of Figs. 13(b), 14(a), and 15(a) show less distortion than the corresponding dotted curves.

Figs. 14(b) and 15(a) show that even the plane lens with only focal length aberration (dotted curve) has the tendency to distort the field into a multiply-humped shape. Theoretical work by E. A. J. Marcatili and further computer simulations have established a periodicity in this behavior. Plane lenses with focal length distortion cause an off-axis field to break up into a double-humped shape which becomes perfectly symmetrical after some distance. After twice this distance the field re-

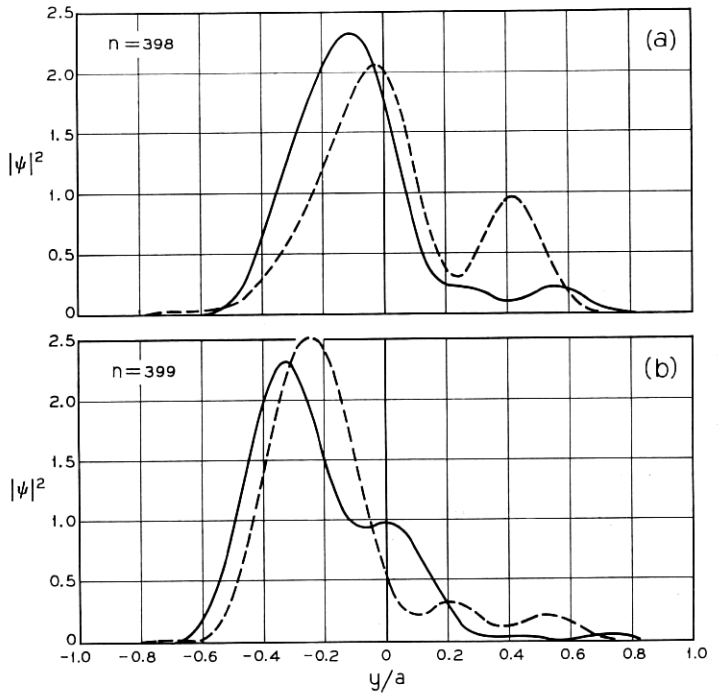

Fig. 15 — Field distortion after 400 lenses. Solid curve, $P = 0.9988$. Dotted curve, $P = 1.0000$.

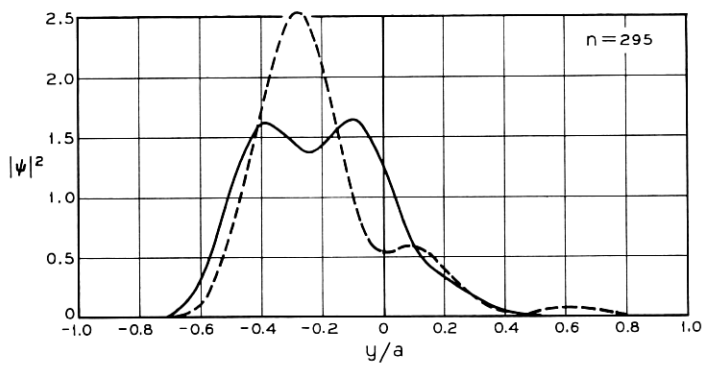

Fig. 16 — The field assumes a double-humped appearance after 295 lenses.

turns to its original shape, etc. No such periodicity seems to exist for distortions caused by a warped principal plane. The periodicity of field distortions caused by focal length aberrations gives a clue to the problem of why so little lens distortion can lead to such serious field distortions. In principle, the field always breaks up into a perfectly symmetric double-humped shape if it is allowed to travel far enough in the beam waveguide. The required distance depends on the amount of focal length aberration but the final field distortion does not. Similarly, it is possible that arbitrarily small distortions of the principal plane may always lead to serious field distortions if given enough length of waveguide. It is still surprising, however, that the slight aberration shown in Fig. 12(a) and 12(b) causes the field to become double humped after only 295 lenses.

REFERENCES

1. Goubau, G. and Schwering, F., On the Guided Propagation of Electromagnetic Wave Beams, IRE Trans., *AP-9*, May, 1961, pp. 248–256.
2. Berreman, D. W., A Lens or Light Guide Using Convectively Distorted Thermal Gradients in Gases, B.S.T.J., *43*, July, 1964, pp. 1469–1475.
3. Marcuse, D. and Miller, S. E., Analysis of a Tuublar Gas Lens, B.S.T.J., *43*, July, 1964, pp. 1741–1758.
4. Marcuse, D., Theory of a Thermal Gradient Gas Lens, IEEE Trans. MTT, *13*, November, 1965, pp. 734–739.
5. Marcuse, D., Comparison Between a Gas Lens and its Equivalent Thin Lens. This issue, pp. 1339–1344.
6. Marcatili, E. A. J., Ray Propagation in Beam Waveguides with Redirectors, B.S.T.J., *45*, January, 1966, pp. 105–115.
7. Courant, R. and Hilbert, D., *Methods of Mathmatical Physics, II*, Interscience Publishers, 1962, p. 317.
8. Fox, A. G. and Li, T., Resonant Modes in a Maser Interferometer, B.S.T.J., *40*, March, 1961, pp. 453–488.
9. Marcuse, D., Physical Limitations on Ray Oscillation Suppressors, B.S.T.J., *45*, May–June, 1966, pp. 743–751.
10. Born, M. and Wolff, E., *Principles of Optics*, Pergamon Press, New York, 1959, p. 112, Equation (15).